LAWRENCE
LIVERMORE
NATIONAL
LABORATORY

UCRL-JRNL-211676

The Impact of Glucuronidation on the Bioactivation and DNA Adduction of the Cooked-Food Carcinogen 2-Amino-1-methyl-6-phenylimidazo[4,5-b] pyridine in vivo

M. A. Malfatti, E. A. Ubick, J. S. Felton

April 25, 2005

Carcinogenesis

The Impact of Glucuronidation on the Bioactivation and DNA Adduction of the Cooked-Food Carcinogen 2-Amino-1-methyl-6-phenylimidazo[4,5-*b*]pyridine *in vivo*

Michael A Malfatti, Esther A. Ubick, and James S. Felton*

Biosciences Directorate, Lawrence Livermore National Laboratory, P.O. Box 808, L-452, Livermore, CA 94551

Key words: Heterocyclic Amines, Glucuronidation, DNA adducts, Metabolism

*To whom correspondence should be addressed

Phone: 925-422-5656

FAX: 925-422-2282

email: felton1@llnl.gov

Abstract

UDP-glucuronosyltransferases (UGTs) catalyze the glucuronidation of many different chemicals. Glucuronidation is especially important for detoxifying reactive intermediates from metabolic reactions, which otherwise can be biotransformed into highly reactive cytotoxic or carcinogenic species. Detoxification of certain food-borne carcinogenic heterocyclic amines (HAs) is highly dependent on UGT1A-mediated glucuronidation. 2-Amino-1-methyl-6-phenylimidazo[4,5-*b*]pyridine (PhIP), the most mass abundant carcinogenic HA found in well-done cooked meat, is extensively glucuronidated by UGT1A proteins. In humans, CYP1A2 catalyzed *N*-hydroxylation and subsequent UGT1A-mediated glucuronidation is a dominant pathway in the metabolism of PhIP. Therefore, changes in glucuronidation rates could significantly alter PhIP metabolism. To determine the importance of UGT1A-mediated glucuronidation in the biotransformation of PhIP, UGT1A proficient Wistar and UGT1A deficient Gunn rats were exposed to a single 100 μg/kg oral dose of [^{14}C]-PhIP. Urine was collected over 24 h and the PhIP urinary metabolite profiles were compared between the two strains. After the 24 h exposure, livers and colon were removed and analyzed for DNA adduct formation by accelerator mass spectrometry. Wistar rats produced several PhIP and *N*-hydroxy-PhIP glucuronides that accounted for ~25% of the total amount of recovered urinary metabolites. In the Gunn rats, PhIP and *N*-hydroxy-PhIP glucuronides were reduced by 68-92%, compared to the Wistar rats, and comprised only 4% of the total amount of recovered urinary metabolites. PhIP-DNA adduct analysis from the Gunn rats revealed a correlation between reduced PhIP and *N*-hydroxy-PhIP glucuronide levels in the urine and increased hepatic DNA adducts, compared to the Wistar rats. These results

indicate that UGT1A-mediated glucuronidation of PhIP and *N*-hydroxy-PhIP is an important pathway for PhIP detoxification. Failure to form glucuronide conjugates results in increases in PhIP bioactivation and DNA adduct formation, which can potentially lead to increases in tumor formation. Therefore, diminished UGT1A activity could pose a significant risk for the development of certain cancers from exposure to PhIP.

Abbreviations

UGT, uridine diphosphate-glucuronosyltransferase; HA, heterocyclic amine; PhIP, 2-amino-1-methyl-6-phenylimidazo[4,5-*b*]pyridine; CYP, cytochrome P450; N-hydroxy-PhIP, 2-hydroxyamino-1-methyl-6-phenylimidazo[4,5-*b*]pyridine; BaP, benzo[*a*]pyrene; NADP, nicotinamide adenine dinucleotide phosphate; UDPGA, uridine diphosphate glucuronic acid; AMS, accelerator mass spectrometry.

Introduction

UDP-glucuronosyltransferase (UGT)-mediated glucuronidation is rapidly becoming recognized as an important pathway in the metabolism of certain food-borne carcinogenic heterocyclic amines (HAs) [1,2]. The UGTs are a superfamily of membrane bound enzymes that catalyze the glucuronidation of many endogenous and xenobiotic compounds. These conjugation reactions are catalyzed by numerous isoforms that have a broad and overlapping substrate selectivity and tissue distribution (*reviewed* in [3]). Glucuronidation is an especially important pathway for detoxifying reactive intermediates from metabolic reactions, which otherwise can be biotransformed into highly reactive cytotoxic or carcinogenic species [4]. The UGT proteins are divided into 2 families based on sequence homologies, designated UGT1 and UGT2 [5]. These families are further divided into three subfamilies, UGT1A, UGT2A, and UGT2B. Studies have shown that the detoxification of certain cooked-food-derived carcinogenic HAs is highly dependent on UGT1A-mediated glucuronide conjugation [1,6-8]. 2-Amino-1-methyl-6-phenylimidazo[4,5-*b*]pyridine (PhIP) is the most mass abundant carcinogenic HA found in well-done cooked meat and is extensively glucuronidated by UGT1A proteins [9-11]. A more recent study, using microsomal preparations from baculovirus infected insect cells containing all the functional UGT1A proteins, has implicated UGT1A1 as the primary UGT1A isoform responsible for glucuronidation of the reactive intermediate of PhIP [8].

Bioactivation of PhIP is highly dependent upon the hepatic cytochrome P4501A2 (CYP1A2) mediated *N*-hydroxylation to the corresponding 2-hydroxyamino-1-methyl-6-phenylimidazo[4,5-*b*]pyridine (*N*-hydroxy-PhIP) [12,13]. *N*-Hydroxy-PhIP is

subsequently esterified by phase II sulfotransferases and/or acetyltransferases that generate the highly electrophilic *O*-sulfonyl and *O*-acetyl esters, respectively. These esters are capable of heterolytic cleavage to generate the reactive nitrenium ion which is considered the ultimate carcinogenic species [14]. The reactive nitrenium ion has been shown to form DNA adducts in multiple tissues [15-17]. UGT1A-mediated *N*-glucuronidation can compete with these activation reactions resulting in the formation of the less reactive *N*-hydroxy-PhIP-N^2-glucuornide and *N*-hydroxy-PhIP-*N*3-glucuonide. These compounds can be excreted through the urine or bile, or can be transported to extrahepatic tissue where deconjugation by β-glucuronidase can occur, leading to the re-generation of the reactive intermediate *N*-hydroxy-PhIP [6,18].

In humans, studies have indicated that CYP1A2 catalyzed *N*-hydroxylation and subsequent UGT1A1-mediated glucuronidation is quantitatively the most important pathway in the metabolism of PhIP. When human volunteers were exposed to PhIP, *N*-hydroxy-PhIP glucuronide conjugates accounted for approximately 60% of the total PhIP urinary metabolites [2]. *N*-hydroxy-PhIP-N^2-glucuronide was also the major metabolite in human urine after consumption of a single cooked chicken meal [19]. Since glucuronidation is such a major contributor to PhIP metabolism, it can be reasoned that changes in glucuronidation rates could significantly alter PhIP metabolism and bioactivation. This concept was reinforced when Chinese hamster ovary cells, that were transfected with the human *UGT1A1* gene, were shown to provide a protective effect against PhIP induced cytotoxicity and mutation induction when compared to control cells that did not contain the *UGT1A1* gene [20].

Polymorphic expression patterns are known to exist for several of the human UGT1A isoforms [21]. These polymorphisms have been implicated as risk factors for certain clinical diseases and cancers due to a reduced capacity to detoxify toxic/carcinogenic compounds [3,22-27]. The most notable polymorphisms are mutations in the *UGT1A1* gene that result in significant down regulation of UGT1A1 activity. Studies using benzo[*a*]pyrene (BaP) have shown that reduced glucuronidation capacity can lead to increases in BaP bioactivation and DNA adduct formation [28-30]. Since PhIP is extensively glucuronidated by UGT1A1 it can be hypothesized that decreases in UGT1A1 expression can lead to increases in PhIP bioactivation and possibly DNA damage.

Most of the studies investigating the differential expression of UGT1A on PhIP metabolism have used *in vitro* techniques. Little has been done, however, to investigate how UGT1A expression affects PhIP bioactivation *in vivo*. The use of the Gunn rat as an *in vivo* model for hepatic UGT1A deficiency has been routinely used to study the effects of reduced hepatic UGT1A activity in the metabolism of various chemicals. The Gunn rat is a mutant strain of the Wistar rat that contains a frame-shift deletion of a single guanosine residue that renders the entire hepatic UGT1A gene locus inactive [31,32]. By using the Gunn rat in this current study it was possible to determine the affect reduced UGT1A activity has on PhIP metabolism *in vivo*. Furthermore, the use of accelerator mass spectrometry (AMS) to analyze DNA adducts, allowed for the use of a human dietary relevant dose of PhIP. Due to low detection limits of many analytical techniques, most animal studies use doses that are 10-100 times higher than what is generally seen in typical human exposures. These traditional limitations have been overcome due to the

extreme sensitivity of AMS. These studies should help provide a better understanding of the overall mechanisms of PhIP biotransformation. Furthermore, understanding how differential UGT1A activity affects PhIP bioactivation may help in evaluating the individual susceptibility to the potential cancer risks from PhIP exposure.

The goal of the current study is to determine what effects reduced UGT1A expression has on PhIP metabolism and DNA adduct formation *in vivo,* and to correlate UGT1A expression levels with DNA adduct levels in certain tumor target tissues. Since the Gunn rat is deficient in the expression of all the hepatic UGT1A isozymes, this study focused on overall UGT1A activity toward PhIP and not any one specific isoform. A decrease in PhIP glucuronide levels in the Gunn rat correlated with an increase in hepatic DNA adducts, compared to the control rats. These findings suggest that diminished UGT1A activity could pose a significant risk for the development of certain cancers from exposure to PhIP.

Materials and Methods

Chemicals

[^{14}C]PhIP was purchased from Toronto Research Chemicals (North York, Ontario, Canada). *N*-hydroxy-PhIP was obtained from SRI International (Palo Alto, CA). The radiochemical purity of [^{14}C]PhIP and the chemical purity of *N*-hydroxy-PhIP were assessed by HPLC (isocratic at 40% methanol) and were determined to be greater than 98% pure for both compounds. Nicotinamide adenine dinucleotide phosphate (NADP), glucose-6-phosphate, glucose-6-phosphate dehydrogenase, β-naphthoflavone, urea, Triton X-100, ribonuclease A and T1, dithiothreitol, and proteinase K were purchased

from Sigma (St. Louis, MO). DNA isolation columns were obtained from Qiagen (Valencia, CA). UDP-glucuronic acid (UDPGA), alamethicin, and all other microsomal reaction buffer components were obtained as a mix from BD Gentest, (Bedford, MA). All immunoblotting reagents were obtained from BioRad, (Hercules, CA.). Antibodies for immunoblotting were obtained from BD Gentest and Santa Cruz Biotechnology, Inc. (Santa Cruz, CA). All other reagents were of analytical grade or better.

Animals

Male Wistar and Gunn rats weighing 200-250 g were obtained from Harlan (Indianapolis, IN). All animals were housed in polystyrene cages containing hardwood bedding and kept on a 12 h light/dark cycle in a ventilated room maintained at 24°C. Animals were allowed to acclimate to their quarters for seven days prior to use for which food (standard lab chow) and water was provided *ad libitum*. In experiments requiring cytochrome P450 and UGT1A induced animals, rats were injected intraperitoneally with β-naphthoflavone at 80 mg/kg in corn oil once a day for three days prior to dosing with [^{14}C]PhIP.

Metabolite and tissue collection

Uninduced and β-naphthoflavone induced animals were administered a single oral gavage dose of 100 μg/kg [^{14}C]PhIP in corn oil containing 1% DMSO v/v (specific activity 14.2 mCi/mmol). The animals were placed in metabolism cages and urine was collected over dry ice for 24 h in 0-4 h and 4-24 h fractions. At 24 h post [^{14}C]PhIP dose, the animals were sacrificed by CO_2 asphyxiation and their livers and colons were removed and stored at -80°C until DNA isolation.

Separation of PhIP metabolites from rat urine

Collected urine was thawed and the total volume of each fraction recorded. A 0.5 ml aliquot from each fraction was analyzed for carbon-14 content by liquid scintillation counting (Wallic, Gaithersburg, MD). Approximately 8000-10,000 DPM of each urine sample was analyzed by reverse-phase HPLC for PhIP and PhIP metabolites by directly injecting the samples onto a Rainin HPLC system (Varian, Walnut Creek, CA) equipped with a 5 μm, 4.6 mm x 150 mm TSK-GEL ODS-80 TM column (Toso Bioscience, Montgomeryville, PA) and monitored at 315 nm. Metabolites were eluted at 0.75 ml/min initially using a solvent of 10% (v/v) methanol/0.1% (v/v) triethylamine, pH 6, for 2 min. This was followed by a gradient to 33% (v/v) methanol/0.1% triethylamine at 32 min, followed by a final gradient to 55% (v/v) methanol/0.1% triethylamine at 60 min. The methanol concentration was maintained at 55% (v/v) from 60 to 70 min. The column eluate was collected at one minute intervals and radioactivity was quantified by scintillation counting.

Microsomal incubations

Microsomes were prepared from both uninduced and β-naphthoflavone induced Wistar and Gunn rat livers by differential centrifugation [33]. Briefly, livers were removed from the animals and homogenized using a Polytron tissue homogenizer (Brinkmann, Westbury, NY) in 3 volumes of ice-cold 0.02 M Tris-HCl buffer containing 1.15% KCl, pH 7.4. The homogenate was centrifuged at 9000 x *g* at 4°C for 20 min. The supernatant was removed and centrifuged again at 100,000 x *g* at 4°C for 1 h. The supernatant was

removed and the microsomal pellet was gently resuspended in 0.1 M Tris-HCl, pH 7.4. The protein concentration was determined by the Bradford method [34]. Microsomal incubations were prepared on ice in 1.5 ml conical plastic tubes. To determine CYP450-mediated PhIP hydroxylation rates, samples consisted of 2.0 mg/ml microsomal protein, 15 mM $MgCl_2$, an NADPH regenerating system (1 mM NADP, 15 mM glucose-6-phosphate, 1U/ml glucose-6-phosphate dehydrogenase), and 10-100 μM PhIP (dissolved in DMSO delivered in 5 μl) in 0.1 M sodium phosphate buffer, pH 7.4, in a total volume of 500 μl. Samples were incubated for 30 min at 37°C. To determine UGT-catalyzed *N*-hydroxy-PhIP glucuronidation rates, samples consisted of 2.0 mg/ml microsomal protein, 8.0 mM $MgCl_2$, 0.5 mM EDTA, 2.0 mM UDPGA, 25 μg/ml alamethicin, and 10-100 μM *N*-hydroxy-PhIP (dissolved in DMSO delivered in 5 μl) in 50 mM Tris-HCl buffer, pH 7.4, in a total volume of 200 μl. Samples were incubated for 3 h at 37°C. After the incubation times, 2 volumes of ice-cold methanol were added to each sample to precipitate the proteins and terminate the reaction. The samples were then allowed to stand at -20° C for 30 min. The protein was then removed by centrifugation in a microcentrifuge at maximum speed for 5 minutes. The methanolic extracts containing the reaction products were placed in clean plastic tubes and stored at -80°C until HPLC analysis.

HPLC analysis of microsomal products

The aqueous-methanol extracts from the microsomal incubations were evaporated to dryness under nitrogen and then reconstituted in 60 μl of HPLC starting mobile phase. The samples were centrifuged in a microcentrifuge for 1 min at maximum speed and 50

μl of supernatant was injected into an Alliance HPLC system (Waters Corp., Milford, MA) equipped with a 5 μm, 4.6 mm x 150 mm TSK-GEL ODS-80 TM column (Toso Bioscience, Montgomeryville, PA) and a Waters 990 photodiode array detector. The metabolites were eluted at 0.75 ml/min using a gradient starting at 30% methanol/0.1% triethylamine, pH 6.0, up to 55% methanol/0.1% triethylamine, pH 6.0, at 8 min. The methanol concentration was maintained at 55% from 8 to 20 min. The identities of the CYP450-mediated PhIP-hydroxy intermediates and the UGT-mediated *N*-hydroxy-PhIP-glucuronide conjugates were confirmed by comparing the HPLC retention time and UV spectra to known metabolite standards. Quantification of each metabolite was based on the molar extinction coefficient of PhIP (19440 $mol^{-1}Lcm^{-1}$ at 315 nm).

Immunoblotting

Western blot analysis was used to confirm the presence/absence of UGT1A proteins in the two rat strains. Immunoblotting was performed according to the manufacturers recommendations (BD Gentest). Briefly, 5-100 μg of microsomal protein from each microsomal preparation was heated at 95° C for 4 min in loading buffer (62.5 mM Tris-HCl, pH 6.8, 2% SDS, 25% glycerol, and 0.01% Bromophenol Blue) containing 2% 2-mercaptoethanol, and then separated on a 10% SDS-polyacrylamide gel. The separated proteins were electrotransferred onto a nitrocellulose membrane. The membrane was blocked in 5% nonfat powdered milk in 25 mM Tris-HCl (pH 7.5), and 150 mM NaCl (solution A) for 1 h, and then washed three times with solution A containing 0.1% Tween 20. The membranes were then incubated for 1 h in 0.5% nonfat powdered milk in solution A containing an antibody (1:500) prepared from a rabbit immunized with a

peptide specific for the conserved carboxyl-terminal region of all UGT1A isoforms (WB-UGT1A; BD Gentest). The membrane was washed three more times and was then incubated for 1 h in 0.5% nonfat powdered milk in solution A containing an HRP-conjugated goat anti-rabbit IgG secondary antibody (1:5000) (Santa Cruz Biotechnology, Inc.), followed by 3 more washings. Visualization was performed using the Immun-Star HP substrate detection kit (BioRad). The identity of the UGT1A protein was based on comparison of the chemiluminescence band to a known UGT1A protein standard (BD Gentest).

DNA isolation and adduct analysis

DNA isolation from rat liver and colon, and sample preparation for the quantification of DNA adduct levels by AMS has been reported elsewhere [35]. Briefly, Tissues were homogenized then digested in lysis buffer [4 M urea, 1.0% Triton X-100, 10 mM EDTA, 100 mM NaCl 10 mM DTT, 10 mM Tris-HCl (pH 8.0)] containing 0.8 mg/ml proteinase K overnight at 37°C. Undigested tissue was removed by centrifugation, and the supernatant was treated for 1 h at room temperature with RNase A, (0.5 mg/ml) and RNase T1 (5 μg/ml). DNA was extracted using Qiagen column chromatography (Qiagen,Valencia, CA) according to the manufacturers instructions. DNA purity was determined by the A260 nm/A280 nm ratio. A ratio between 1.6-1.8 was considered pure. Pure DNA samples were then submitted for adduct analysis by AMS.

Results

Recovery of urinary metabolites

The total amount of radioactivity recovered in the urine over the 24 h collection period was similar in the two rat strains. Over 24 h, 13-16% of the administered dose was recovered in the urines of both the Wistar and Gunn rats. Induction with β-naphthoflavone did not change the amount of overall radioactivity excreted, however, the rate of excretion was different in the two strains. In the Wistar rats approximately 50% of the recovered radioactivity was excreted in the first 4 h of collection in both the induced and uninduced animals (Figure 1). In the uninduced Gunn rats 60% of the recovered radioactivity was excreted in the first 4 h, and in the β-naphthoflavone induced Gunn rats over 70% of the recovered radioactivity was excreted in the first 4 h.

Chromatographic analysis of the urine from β-naphthoflavone induced Wistar rats revealed eight relevant radioactive peaks (Figure 2A). Based on co-elution with authentic PhIP metabolite standards five of the peaks have been positively identified. The major peak, at a retention time of 33 min, co-eluted with a 4'-PhIP-sulfate authentic standard. The peaks at 31 min and 52 min were determined to be 4'-O-PhIP-glucuronide and *N*-hydroxy-PhIP-*N*3-glucuronide, respectively. The peak at 60 min co-eluted with an *N*-hydroxy-PhIP standard. This peak was observed only in the 0-4 h urine fraction. The parent compound PhIP was detected at 62 min. Based on electrospray ionization-mass spectral characterization, the peak at 22 min produced molecular ions at *m/z* 401 $[M+H]^+$ and upon collision induced dissociation produced fragment ions at *m/z* 225 $[M+H]^+$ which is consistent with a direct PhIP-glucuronide. The radioactivity between 44-47 min was unresolvable by HPLC, however, MS/MS analysis of these peaks revealed molecular

ions at *m/z* 417 $[M+H]^+$ and fragment ions at *m/z* 241 $[M+H]^+$ and *m/z* 225 $[M+H]^+$. The fragmentation pattern was identical to what has been seen for *N*-hydroxy-PhIP-N^2-glucuronide [6]. Molecular parent ions of *m/z* 241 $[M+H]^+$ were also detected indicating the presence of a hydroxy-PhIP metabolite. Both *N*-hydroxy-PhIP-N^2-glucuronide and 4'-hydroxy-PhIP standards co-eluted at approximately 44 min on the HPLC. The peak that eluted at 36-37 min was not identified. In the uninduced Wistar rats, the levels of all detectable metabolites were decreased by approximately 10% compared to the induced animals (data not shown).

The urinary PhIP metabolic profile in the Gunn rats was significantly different from what was observed in the Wistar rats (Figure 2B). The levels of all the PhIP and *N*-hydroxy-PhIP glucuronide conjugates were dramatically reduced in the Gunn rat compared to the Wistar rat. In the β-naphthoflavone induced Gunn rats *N*-hydroxy-PhIP-*N*3-glucuronide, the direct PhIP-glucuronide, and 4'-O-PhIP-glucuornide were reduced by 92%, 75%, and 68%, respectively, compared to the glucuronide conjugate levels in the Wistar rats (Figure 3). Similar reductions were also seen in the uninduced animals. In the Wistar rats all the PhIP and *N*-hydroxy-PhIP glucuronide conjugates accounted for 18 and 25% of the urinary metabolites in the uninduced and induced animals, respectively. Whereas, in the Gunn rats the PhIP and *N*-hydroxy-PhIP glucuronides accounted for only 2.5%-4.0% of the total amount of recovered metabolites (Figure 3). Interestingly, the reduction of glucuronide conjugate formation in the Gunn rats did not result in the increase in any of the other detected metabolites. These results clearly demonstrate that the Gunn rat has a diminished capacity to form PhIP and *N*-hydroxy-PhIP glucuronides.

Microsomal metabolism

To ensure cytochrome P450 hydroxylation rates were consistent between the two rat strains, hepatic microsomes were prepared from each strain and exposed to PhIP. NADPH-dependent metabolism of PhIP was assessed in each microsomal preparation. There was no difference in CYP450 mediated hydroxylation rates of PhIP between the two rat strains (data not shown). Microsomes from both the Wister and the Gunn rats produced both 4'-hydroxy-PhIP and *N*-hydroxy-PhIP. 4'-Hydroxy-PhIP was formed at a rate approximately 2 times faster than *N*-hydroxy-PhIP.

To assess hepatic UDP-glucuronosyltransferase rates, *N*-hydroxy-PhIP was exposed to both Wistar and Gunn liver microsomes that were fortified with UDPGA. The microsomes prepared from the Wistar rats produced both *N*-hydroxy-PhIP-N^2-glucuronide and *N*-hydroxy-PhIP-*N*3-glucuronide (Figure 4). *N*-hydroxy-PhIP-*N*3-glucuronide was produced at a rate seven times faster than *N*-hydroxy-PhIP-N^2-glucuronide. In the microsomes prepared from the Gunn rats the formation of *N*-hydroxy-PhIP-N^2-glucuornide was reduced nearly 10 fold compared to the rate of formation observed in the microsomes derived from the Wistar rats. Unexpectedly, the rate of formation of *N*-hydroxy-PhIP-*N*3-glucuronide was similar to the rate seen in the Wistar rat derived microsomes (Figure 4).

Immunoblotting

To confirm the presence/absence of hepatic UGT1A protein expression in each rat strain Western blot analysis was performed on the microsomal extracts from both the Wistar and Gunn rats. The antibody used was a polyclonal anti-human UGT1A peptide raised in

a rabbit that is specific for the carboxyl terminus of the protein, whose sequence is conserved for human and rat for all UGT1A proteins [36]. Since this peptide will react with all of the UGT1A isoforms it was not possible to determine the expression levels of the individual UGT1A isozymes. The microsomes isolated from the β-naphthoflavone induced Wistar rats revealed the presence of a protein with a molecular mass of approximately 54 kDa, which was identical to the UGT1A protein standard (Figure 5). No protein band could be detected from the samples from the uninduced animals. These findings indicate there was an increase in UGT1A protein expression due to β-naphthoflavone treatment. There was no evidence of UGT1A protein expression from the microsomes derived from the Gunn rats (Figure 5).

DNA adduct analysis

DNA adducts were detected, by AMS analysis, in the livers and colons of all animals that were treated with a single oral dose of [^{14}C]PhIP (Table I). In the liver, adducts were detected in the β-naphthoflavone induced UGT1A proficient Wistar rats at 268.6 ± 63.8 adducts/10^{12} nucleotides. Adduct levels from the UGT1A deficient Gunn rats with similar treatment were five times higher at 1051.8 ± 251.9 adducts/10^{12} nucleotide. In the uninduced animals adduct levels in the livers were 847.8 ±114.5 and 996.1 ± 205.9 adducts/10^{12} nucleotide in the Wistar and Gunn rats respectively. DNA adducts in the colons of the β-naphthoflavone induced Wistar and Gunn rats were 7 and 8 times lower than what was observed in the colons of the uninduced animals respectively, indicating that inducible UGT1A activity in the colon of both strains was capable of detoxifying the *N*-hydroxy-PhIP reactive intermediate. These results suggest that UGT1A proteins may

play a role in the detoxification of PhIP since the animals that were deficient in hepatic UGT1A produced more liver DNA adducts than the UGT1A proficient animals.

Discussion

The use of the Gunn rat as a model for UGT1A deficiency has allowed for comparisons with the UGT1A proficient Wistar rats as to the impact UGT1A expression has on PhIP bioactivation and DNA adduct formation. However, since the metabolism of PhIP in rodents is different than what has been reported for humans [37], the results obtained in this present study can only be used as an indicator as to what may occur in humans. Nevertheless, in humans *N*-glucuronidation of *N*-hydroxy-PhIP is a major pathway in the overall metabolism of PhIP, whereas, in rodents this pathway is not as dominant [2]. Therefore, the effects of UGT activity on PhIP metabolism may be more dramatic in humans compared to what has been observed in these rat studies. Furthermore, by using AMS technology to detect DNA adducts, the affects from PhIP exposure can be assessed at a human dietary relevant dose. The 100 μg/kg PhIP dose used is equivalent to the dose one would generally receive from the consumption of one well-done cooked chicken breast [38].

The dramatic decrease in all the PhIP and *N*-hydroxy-PhIP glucuronides in the urine of the Gunn rats clearly demonstrates that glucuronidation plays a major role in the metabolism of PhIP. In the β-naphthoflavone induced Wistar rats, PhIP and *N*-hydroxy-PhIP glucuronides accounted for approximately 25% of all the recovered metabolites. Whereas, in the Gunn rats only 4% of the metabolites were glucuronide conjugates. Interestingly, this 84% reduction in glucuronides did not cause an increase in any of the

other detected urinary metabolites. These findings are in contrast to a previous study that reported increases in several PhIP metabolites in the urine of Gunn rats after an intravenous (iv) PhIP exposure, and a 2 h urine collection [39]. In that study the only metabolite that was decreased was *N*-hydroxy-PhIP-*N*3-glucuonide. The discrepancies between the previous and this current study could be due to the differences in dosing methods and urine collection times. By using an iv exposure route the distribution of PhIP would be much quicker compared to an oral exposure, however, an iv exposure would also bypass first pass metabolism. Since human exposure to PhIP is predominantly oral, first pass metabolism could be a significant contributor to the overall biotransformation of PhIP.

The lack of compensatory changes in non-glucuronide PhIP metabolites in the Gunn rats despite decreases in the PhIP and *N*-hydroxy-PhIP glucuronide conjugates was somewhat unexpected. However, since the greatest metabolite reduction was from *N*-hydroxy-PhIP-*N*3-glucuronide it is possible that increases could have occurred in *N*-hydroxy-PhIP and its subsequent bioreactive acetoxy and sulfoxy derivatives. Due to their high reactivity, these compounds would not have been detected in the urine. Evidence for this concept was observed from the DNA adduct data. The increase in DNA adducts in the livers of the Gunn rats positively correlated with a decrease in *N*-hydroxy-PhIP-*N*3-glucurornide levels in the urine indicating an increase in PhIP bioactivation compared to the Wistar rats. Similar results were obtained from Gunn rats exposed to BaP [28]. Enhanced covalent binding of BaP to hepatic DNA and microsomal protein was correlated with a deficiency in BaP glucuronidation compared to control rats with normal UGT activity.

Induction with β-naphthoflavone had a significant effect on DNA adduct levels in both rat strains. The 3-fold decrease in DNA adducts observed in the liver, and the 7-fold decrease observed in the colon of the β-naphthoflavone induced Wistar rats compared to the uninduced animals suggests that inducible UGT1A activity contributes to the detoxification of the *N*-hydroxy-PhIP reactive intermediate. The larger decrease seen in the colon compared to the liver could be due to the presence of a more diverse spectrum of UGT1A isoforms in the colon that are capable of glucuronidating *N*-hydroxy-PhIP [8]. The higher adduct levels seen in the colon of the uninduced Wistar rats compared to the liver could be due to enterohepatic circulation of *N*-hydroxy-PhIP. More of the reactive compound would be entering the colon and without UGT1A induction the ability to detoxify it would be diminished. The 8-fold decrease in DNA adducts in the colon of the β-naphthoflavone Gunn rats compared to the liver is another indicator of the importance of UGT1A-mediated detoxification of *N*-hydroxy-PhIP. Since the Gunn rat is deficient in hepatic UGT1A activity, more DNA adducts were formed in the liver due to the inability to form N-hydroxy-PhIP glucuronides. However, in the colon, where UGT1A activity is present, adduct levels were significantly lower indicating UGT1A-mediated detoxification of *N*-hydroxy-PhIP takes place in the colon but not the liver.

Based on these results, Figure 6 represents a proposed schematic as to the metabolic fate of PhIP and the effect of UGT1A activity on PhIP bioactivation in both the Wistar and Gunn rats. After oral ingestion, PhIP enters the gut where it is transported to the liver and converted via CYP1A2 to *N*-hydroxy-PhIP. In the β-naphthoflavone induced Wistar rat the increase in hepatic UGT activity would be capable of forming *N*-hydroxy-PhIP glucuronides, which are readily excreted through the urine or transported

to the colon and excreted. Remaining *N*-hydroxy-PhIP would be further bioactivated to form low levels of DNA adducts in both the liver and colon. In the uninduced Wistar rat, where the UGT1A levels are lower, *N*-hydroxy-PhIP would be the predominant metabolite, which would result in the formation of DNA adducts in the liver and colon at higher levels than what was seen in the induced animals (Figure 6A). In the β-naphthoflavone induced Gunn rat the fate of PhIP would be different (Figure 6B). Since the Gunn rat is deficient in hepatic UGT1A activity, *N*-hydroxy-PhIP would predominate in the liver leading to increased DNA adduct levels due to the inability to form *N*-hydroxy-PhIP-glucuronides. In the colon, however, induced UGT1A activity would be sufficient to glucuronidate *N*-hydroxy-PhIP leading to detoxification over bioactivation (Figure 6B). In the uninduced Gunn rat the fate of PhIP would be similar to what was proposed for the uninduced Wistar rat. These proposed pathways demonstrate the importance of UGT1A activity in the biotransformation of PhIP.

The formation of *N*-hydroxy-PhIP-*N*3-glucuronide in the microsomal incubations derived from the UGT1A deficient rats at levels comparable to the UGT1A proficient rats was unexpected. This finding was significantly different from what was observed in the urinary metabolic profile where *N*-hydoxy-PhIP-*N*3-glucuronide was decreased by 92% in the UGT1A deficient rats compared to the control animals. It is unclear why the *in vivo* data was so different from the microsomal data. These differences could be due to the involvement of other UGT isozymes and/or competition by other enzymatic pathways. This idea was reinforced from the Western blot analysis of the hepatic microsomal fractions that showed no presence of UGT1A proteins in the Gunn rats. It is possible that UGT enzymes from the 2B subfamily are involved in the formation of *N*-

hydroxy-PhIP-*N*3-glucuornide. However, in the *in vivo* situation, other phase II enzymes such as acetyltransferase and sulfotransferase may have a higher affinity for the *N*-hydroxy-PhIP substrate over the UGT2B enzymes. This increased affinity would out-compete UGT2B for the substrate and lead to the formation of bioreactive esters instead of UGT2B-mediated *N*-hydroxy-PhIP-*N*3-glucuronide. In the microsomal reactions there is no competition since the other phase II enzymes are found in the soluble fraction of the cells. Therefore, in the microsomal reaction the UGT2B enzymes can react freely with *N*-hydroxy-PhIP to form *N*-hydroxy-PhIP-*N*3-glucuronide. This theory remains to be proven.

The results from these studies indicate that UGT1A-mediated glucuronidation of PhIP and *N*-hydroxy-PhIP is an important pathway in the detoxification of PhIP. The failure to form glucuronide conjugates can lead to increases in PhIP bioactivation and DNA adduct formation, as evidenced by the increase in hepatic DNA adducts in the Gunn rats. Increases in DNA adduct formation can potentially lead to increases in tumor formation. These findings suggest that individuals with reduced UGT1A activity would have a higher rate of PhIP activation and be more inclined to form DNA adducts compared to individuals with normal UGT1A activity. Therefore, diminished UGT1A activity could pose a significant risk for the development of certain cancers from exposure to PhIP. Reduced UGT1A activity in humans has been associated with several *UGT1A* gene polymorphism. These polymorphisms have been shown to occur in a significant percentage of the general population (3-10%) (*reviewed in* [21]). Consequently, low UGT1A activity and the concomitant increases in PhIP bioactivation and DNA adduct formation can potentially be a significant risk factor when assessing the

tumorigenic effects from PhIP exposure. It is hoped that these findings will serve as a basis for future studies to better assess individual susceptibility to the potential cancer risk from exposure to PhIP, as well as, other heterocyclic amines.

Acknowledgements

The Authors would like to thank Mark Knize for his analysis of the PhIP metabolites by LC/MS. This work was performed under the auspices of the U.S. Department of Energy by the University of California, Lawrence Livermore National Laboratory under contract No. W-7405-Eng-48, and supported by NCI Grant CA55861.

References

1. Turesky, R.J., Garner, R.C., Welti, D.H., Richoz, J., Leveson, S.H., Dingley, K.H., Turteltaub, K.W. and Fay, L.B. (1998) Metabolism of the food-borne mutagen 2-amino-3,8-dimethylimidazo[4,5-*f*]quinoxaline in humans. *Chemical Research in Toxicology*, **11**, 217-225.

2. Malfatti, M.A., Kulp, K.S., Knize, M.G., Davis, C., Massengill, J.P., Williams, S., Nowell, S., MacLeod, S., Dingley, K.H., Turteltaub, K.W., Lang, N.P. and Felton, J.S. (1999) The identification of [2-^{14}C]2-amino-1-methyl-6-phenylimidazo[4,5-*b*]pyridine metabolites in humans. *Carcinogenesis*, **20**, 705-713.

3. Tukey, R.H. and Strassburg, C.P. (2000) Human UDP-glucuronosyltransferases: Metabolism, Expression, Disease. *Annu. Rev. Pharmacol. Toxicol.*, **40**, 581-616.

4. Dutton, G.J. (1980) *Glucuronidation of drugs and other compounds*. CRC Press, Boca Raton.

5. Mackenzie, P.I., Owens, I.S., Burchell, B., Bock, K.W., Bairoch, A., Belanger, A., Fournel-Gigleux, S., Green, M., Hum, D.W., Iyanagi, T., Lancet, D., Louisot, P., Magdalou, J., Chowdhurry, J.R., Ritter, J.K., Schachter, H., Tephly, T.R., Tipton, K.F. and Nebert, D.W. (1997) The UDP-glycosyltransferase gene superfamily: recommended nomenclature update based on evolutionary divergence. *Pharmocogenetics*, **7**, 255-269.

6. Kaderlik, K.R., Mulder, G.J., Turesky, R.J., Lang, N.P., Teitel, C.H., Chiarelli, M.P. and Kadlubar, F.F. (1994) Glucuronidation of N-hydroxy heterocyclic amines by human and rat liver microsomes. *Carcinogenesis*, **15**, 1695-1701.

7. Stillwell, W.G., Turesky, R.J., Sinha, R. and Tannenbaum, S.R. (1999) N-Oxidative metabolism of 2-amino-3,8-dimethylimidazo[4,5-*f*]quinoxaline (MeIQx) in humans: Excretion of the N^2-glucuronide conjugate of 2-hydroxyamino-MeIQx in urine. *Cancer Res.*, **59**, 5154-5159.

8. Malfatti, M.A. and Felton, J.S. (2004) Human UDP-glucuronosyltransferase 1A1 is the primary enzyme responsible for the N-glucuronidation of N-hydroxy-PhIP in vitro. *Chemical Research in Toxicology*, **17**, 1137-1144.

9. Nowell, S.A., Massengill, J.S., Williams, S., Radominska-Pandya, A., Tephly, T.R., Cheng, Z., Strassburg, C.P., Tukey, R.H., MacLeod, S.L., Lang, N.P. and Kadlubar, F.F. (1999) Glucuronidation of 2-hydroxyamino-1-methyl-6-phenylimidazo[4, 5-b]pyridine by human microsomal UDP-glucuronosyltransferases: identification of specific UGT1A family isoforms involved. *Carcinogenesis*, **20**, 1107-14.

10. Yueh, M.-F., Nguyen, N., Famourzadeh, M., Strassburg, C.P., Oda, Y., Guengerich, P.F. and Tukey, R.H. (2001) The contribution of UDP-glucuronosyltransferase 1A9 on CYP1A2-mediated genotoxicity by aromatic and heterocyclic amines. *Carcinogenesis*, **22**, 943-950.

11. Malfatti, M.A. and Felton, J.S. (2001) *N*-Glucuronidation of 2-amino-1-methyl-6-phenylimidazo[4,5-*b*]pyridine (PhIP) and *N*-hydroxy-PhIP by specific human UDP-glucuronosyltransferases. *Carcinogenesis*, **22**, 1087-1093.

12. Edwards, R.J., Murray, B.P., Murray, S., Schulz, T., Neubert, D., Gant, T.W., Thorgeirsson, S.S., Boobis, A.R. and Davies, D.S. (1994) Contribution of CYP1A1 and CYP1A2 to the activation of heterocyclic amines in monkeys and humans. *Carcinogenesis*, **15**, 829-836.

13. Boobis, A.R., Lynch, A.M., Murray, S., de la Torre, R., Solans, A., Farre, M., Segura, J., Gooderham, N.J. and Davies, D.S. (1994) CYP1A2-catalyzed conversion of dietary heterocyclic amines to their proximate carcinogens is their major route of metabolism in humans. *Cancer Research*, **54**, 89-94.

14. Kato, R. and Yamazoe, Y. (1987) Metabolic activation and covalent binding to nucleic acids of carcinogenic heterocyclic amines from cooked foods and amino acid pyrolysates. *Japan Journal of Cancer Research*, **78**, 297-311.

15. Buonarati, M.H., Turteltaub, K.W., Shen, N.H. and Felton, J.S. (1990) Role of sulfation and acetylation in the activation of 2-amino-1-methyl-6-phenylimidazo[4,5-b]pyridine to intermediates which bind DNA. *Mutation Research*, **245**, 185-190.

16. Nagaoka, H., Wakabayashi, K., Kim, S.B., Kim, I.S., Tanaka, Y., Ochiai, M., Tada, A., Nukaya, H., Sugimura, T. and Nagao, M. (1992) Adduct formation at C-8 of guanine on in vitro reaction of the ultimate form of 2-amino-1-methyl-6-phenylimidazo[4,5-*b*]pyridine with 2'-deoxyguanosine and its phosphate esters. *Japan Journal of Cancer Research*, **83**, 1025-1029.

17. Ozawa, S., Chou, H.-C., Kadlubar, F.F., Nagata, K., Yamazoe, Y. and Kato, R. (1994) Activation of 2-hydroxyamino-1-methyl-6-phenylimidazo[4,5-*b*]pyridine by cDNA-expressed human and rat arylsulfotransferases. *Japan Journal of Cancer Research*, **85**, 1220-1228.

18. Alexander, J., Wallin, H., Rossland, O.J., Solberg, K., Holme, J.A., Becher, G., Andersson, R. and Grivas, S. (1991) Formation of a glutathione conjugate and a semistable transportable glucuronide conjugate of N2-oxidized species of 2-amino-1-methyl-6-phenylimidazo[4,5-*b*]pyridine (PhIP) in rat liver. *Carcinogenesis*, **12**, 2239-2245.

19. Kulp, K.S., Knize, M.G., Malfatti, M.A., Salmon, C.P. and Felton, J.S. (2000) Identification of urine metabolites of 2-amino-1-methyl-6-phenylimidazo[4,5-

b]pyridine following consumption of a single cooked chicken meal in humans. *Carcinogenesis*, **21**, 2065-2072.

20. Malfatti, M.A., Wu, R.W. and Felton, J.S. (2005) The effect of UDP-glucuronosyltransferase 1A1 expression on the mutagenicity and metabolism of the cooked-food carcinogen 2-amino-1-methyl-6-phenylimidazo[4,5-b]pyridine in CHO cells. *Mutation Research*, **570**, 205-214.

21. Guillemette, C. (2003) Pharmacogenomics of human UDP-glucuronosyltransferase enzymes. *The Pharmacogenomics Journal*, **3**, 136-158.

22. Grant, D.J. and Bell, D.A. (2000) Bilirubin UDP-glucuronosyltransferase 1A1 gene polymorphisms: Susceptibility to oxidative damage and cancer. *Molecular Carcinogenesis*, **29**, 198-204.

23. Strassburg, C.P., Vogel, A., Kneip, S., Tukey, R.H. and Manns, M.P. (2002) Polymorphisms of the human UDP-glucuronosyltransferase (UGT) 1A7 gene in colorectal cancer. *Gut*, **50**, 851-856.

24. Minors, J.O., McKinnon, R.A. and Mackenzie, P.I. (2002) Genetic polymorphisms of UDP-glucuronosyltransferase and their functional significance. *Toxicology*, **181-182**, 453-456.

25. Ockenga, J., Vogel, A., Teich, N., Keim, V., Manns, M.P. and Strassburg, C.P. (2003) UDP-glucuronosyltransferase (UGT1A7) gene polymorphisms increase the risk of chronic pancreatitis and pancreatic cancer. *Gastroenterology*, **124**, 1802-1808.

26. Burchell, B. (2003) Genetic variation of human UDP-glucuronosyltransferase: implications in disease and drug glucuronidation. *American Journal of Pharmacogenomics*, **3**, 37-52.

27. Adegoke, O.J., Shu, X.O., Gao, Y.T., Cai, Q., Breyer, J., Smith, J. and Zheng, W. (2004) Genetic polymorphisms in uridine diphospho-glucuronosyltransferase 1A1 (UGT1A1) and risk of breast cancer. *Breast Cancer Research and Treatment*, **85**, 239-245.

28. Hu, Z. and Wells, P.G. (1992) In vitro and in vivo biotransformation and covalent binding of benzo(a)pyrene in Gunn and RHA rats with a genetic deficiency in bilirubin uridine diphosphate-glucuronosyltransferase. *The Journal of Pharmacology and Experimental Therapeutics*, **263**, 334-342.

29. Hu, Z. and Wells, P.G. (2004) Human interindividual variation in lymphocyte UDP-glucuronosyltransferases as a determinant of in vitro benzo[a]pyrene covalent binding and cytotoxicity. *Toxicological Sciences*, **78**, 32-40.

30. Fang, J.-L. and Lazarus, P. (2004) Correlation between the UDP-glucuronosyltransferase (UGT1A1) TATAA box polymorphism and carcinogen detoxification phenotype: Significantly decreased glucuronidating activity against benzo(a)pyrene-7,8-dihydrodiol(—) in liver microsomes from subjects with the UGT1A1*28 variant. *Cancer Epidemiology, Biomarkers and Prevention*, **13**, 102-109.

31. Roy-Chowdhury, J., Huang, T., Kesari, K., Lederstein, M., Arias, I.M. and Roy-Chowdhury, N. (1991) Molecular basis for the lack of bilirubin-specific and 3-methylcholanthrene-inducible UDP-glucuronosyltransferase activities in Gunn rats. *The Journal of Biological Chemistry*, **266**, 18294-18298.

32. Iyanagi, T., Watanabe, T. and Uchiyama, Y. (1989) The 3-methylcholanthrene-inducible UDP-glucuronosyltransferase deficiency in the hyperbilirubinemic rat (Gunn rat) is caused by a -1 frameshift mutation. *Journal of Biological Chemistry*, **264**, 21302-21307.

33. Buonarati, M.H. and Felton, J.S. (1990) Activation of 2-amino-1-methyl-6-phenylimidazo[4,5-*b*]pyridine (PhIP) to mutagenic metabolites. *Carcinogenesis*, **11**, 1133-1138.

34. Bradford, M.M. (1976) A rapid and sensitive method for the quantification of microgram quantities of protein utilizing the principle of protein-dye binding. *Anal. Biochem.*, **72**, 248-254.

35. Dingley, K.H., Ubick, E.A., Vogel, J.S. and Haack, K.W. (2004) DNA isolation and sample preparation for quantification of adduct levels by accelerator mass spectrometry. In Keohavong, P. and Grant, S.G. (eds.), *Methods Mol. Biol.* Humana Press Inc., vol. 291, pp. 21-27.

36. King, C.D., Green, M.D., Rios, G.R., Coffman, B.L., Owens, I.S., Bishop, W.P. and Tephly, T.R. (1996) The glucuronidation of exogenous and endogenous compounds by stably expressed rat and human UDP-glucuronosyltransferase 1.1. *Archives of Biochemistry and Biophysics*, **332**, 92-100.

37. Turteltaub, K.W., Dingley, K.H., Curtis, K.D., Malfatti, M.A., Turesky, R.J., Garner, R.C., Felton, J.S. and Lang, N.P. (1999) Macromolecular adduct formation and metabolism of heterocyclic amines in humans and rodents at low doses. *Cancer Letters*, **143**, 149-156.

38. Sinha, R., Rothman, N., Brown, E.D., Salmon, C.P., Knize, M.G., Swanson, C.A., Rossi, S.C., Mark, S.D., Levander, O.A. and Felton, J.S. (1995) High concentrations of the carcinogen 2-amino-1-methyl-6-phenylimidazo[4,5-*b*]pyridine (PhIP) occur in chicken but are dependent on the cooking method. *Cancer Research*, **55**, 4516-4519.

39. Dietrich, C.G., Ottenhoff, R., de Waart, D.R. and Oude Elferink, R.P.J. (2001) Lack of UGT1 isoform in Gunn rats changes metabolic ratio and facilitates excretion of the food-derived carcinogen 2-amino-1-methyl-6-phenylimidazo[4,5-*b*]pyridine. *Toxicology and Applied Pharmacology*, **170**, 137-143.

Table I. DNA adducts from Wistar and Gunn rats that were exposed to a single oral dose of [^{14}C]PhIP[a]

Tissue	Wistar BNF induced	Gunn BNF induced	Wistar uninduced	Gunn uninduced
Liver	268.6 ± 63.8[b]	1051.8 ± 251.9	847.8 ± 114.5	996.1 ± 205.9
Colon	326.4 ± 40.03	129.5 ± 13.5	2118.6 ± 295.9	1045.7 ± 229.6

[a][^{14}C]PhIP dose was 100 μg/kg

[b]Data is expressed as adducts/10^{12} nucleotides and is the mean ± SE of 4 animals.

Figure Legends

Figure 1. Urinary excretion of [^{14}C]-PhIP in β-naphthoflavone (BNF) induced and uninduced Wistar and Gunn rats over time. Urine was collected over 24 h, divided into 2 fractions: ▒ 0-4h fraction; ■ 4-24 h fraction. Data is the mean of 4 animals ± S.D.

Figure 2. HPLC radio-profile of urine from β-naphthoflavone induced rats exposed to a single oral dose of 100 μg/kg [^{14}C]PhIP. Urine was collected over 24 h. A: UGT1A proficient Wistar rats; B: UGT1A deficient Gunn rats.

Figure 3. Difference in urinary PhIP metabolite levels from UGT1A proficient Wistar rats and UGT1A deficient Gunn rats exposed to a single oral dose of 100 μg/kg [^{14}C]PhIP. ▒ Wistar rat; ■ Gunn rat. Data is the mean of 4 animals ± S.D.

Figure 4. UDP-glucuronosyltransferase-mediated glucuronidation of *N*-hydroxy-PhIP from hepatic microsomes prepared from Wistar (solid line) and Gunn (dashed line) rats. Data is the mean of 3 incubations ± S.D.

Figure 5. Western blot of UGT1A from hepatic microsomal preparations from Wistar and Gunn rats. The antibody is specific for the carboxyl-terminal region of the protein, which is conserved for all UGT1A proteins. The protein bands at approximately 52 kDa represent all UGT1A subfamily members.

Figure 6. Proposed schematic of the metabolic fate of PhIP and the effect of UGT1A activity on PhIP bioactivation in A; Wistar, and B: Gunn rats. Thick lines represent the predominant pathway. See text for further explanation.

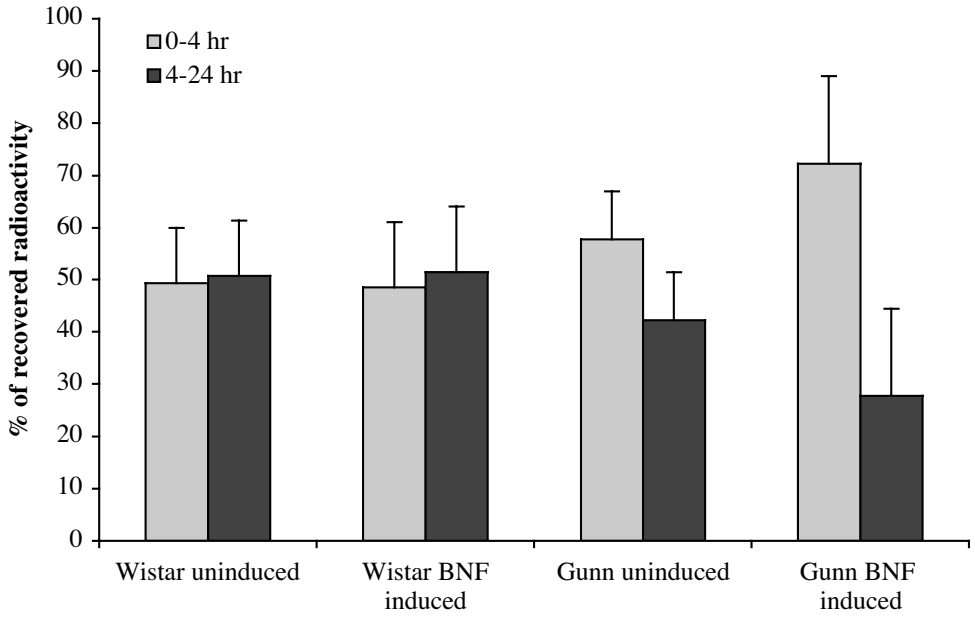
100
90
80
70
60
50
40
30
20
10
0
0-4 hr
4-24 hr
% of recovered radioactivity
Wistar uninduced
Wistar BNF induced
Gunn uninduced
Gunn BNF induced

Figure 1

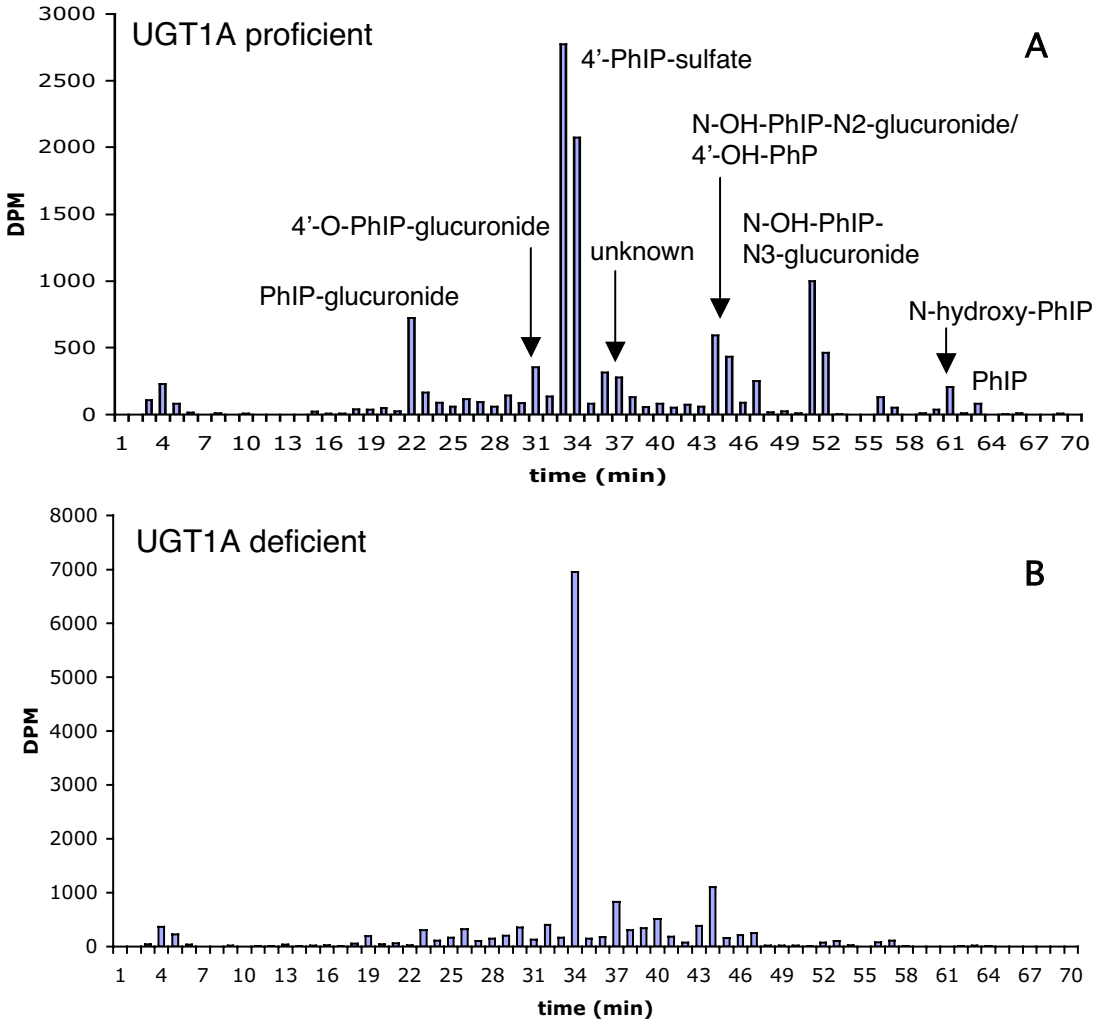
UGT1A proficient
A
4'-PhIP-sulfate
N-OH-PhIP-N2-glucuronide/
4'-OH-PhP
4'-O-PhIP-glucuronide
unknown
N-OH-PhIP-
N3-glucuronide
PhIP-glucuronide
N-hydroxy-PhIP
PhIP
DPM
time (min)
UGT1A deficient
B
DPM
time (min)

Figure 2

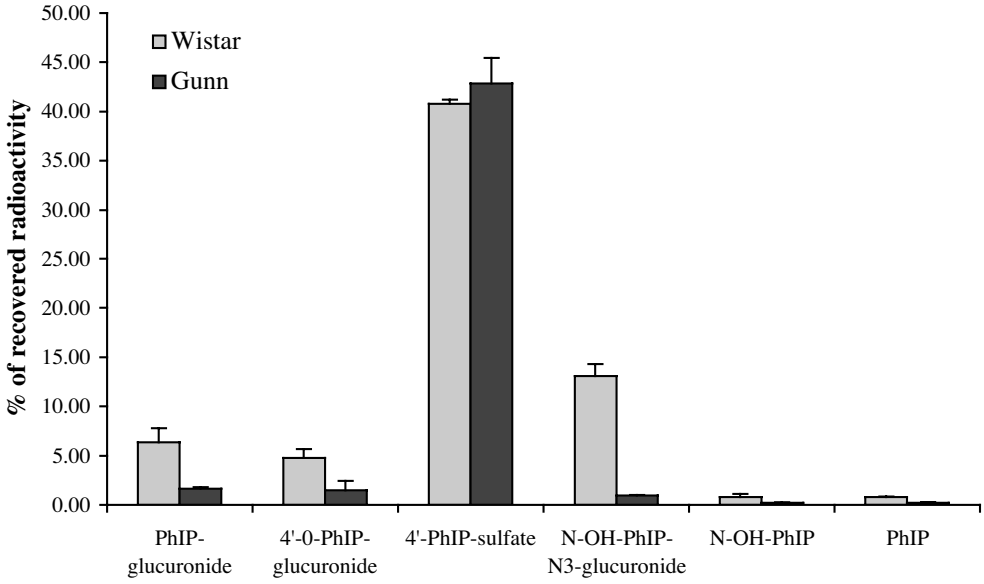
50.00
45.00
40.00
35.00
30.00
25.00
20.00
15.00
10.00
5.00
0.00
% of recovered radioactivity
Wistar
Gunn
PhIP-glucuronide
4'-0-PhIP-glucuronide
4'-PhIP-sulfate
N-OH-PhIP-N3-glucuronide
N-OH-PhIP
PhIP

Figure 3

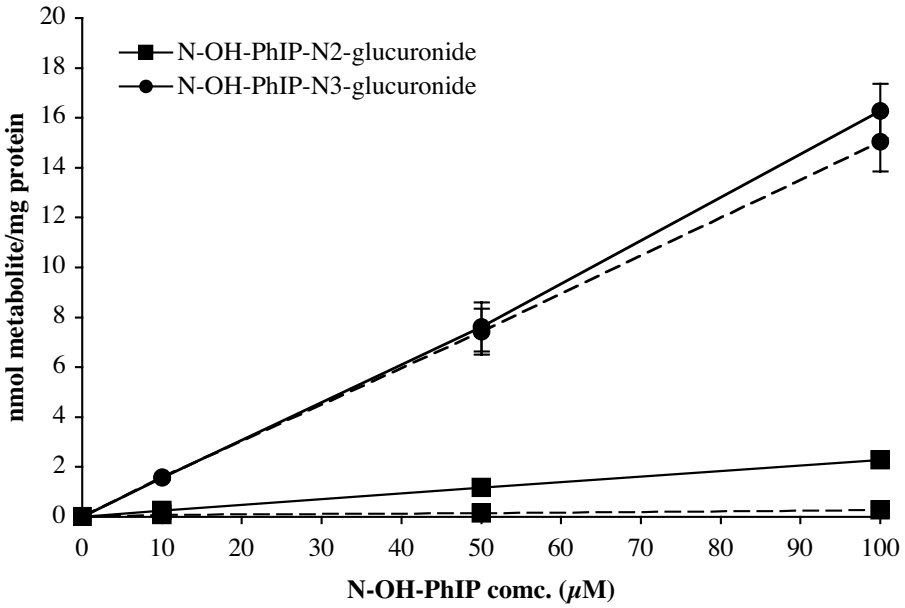
N-OH-PhIP-N2-glucuronide
N-OH-PhIP-N3-glucuronide
nmol metabolite/mg protein
N-OH-PhIP comc. (μM)
0
2
4
6
8
10
12
14
16
18
20
0
10
20
30
40
50
60
70
80
90
100

Figure 4

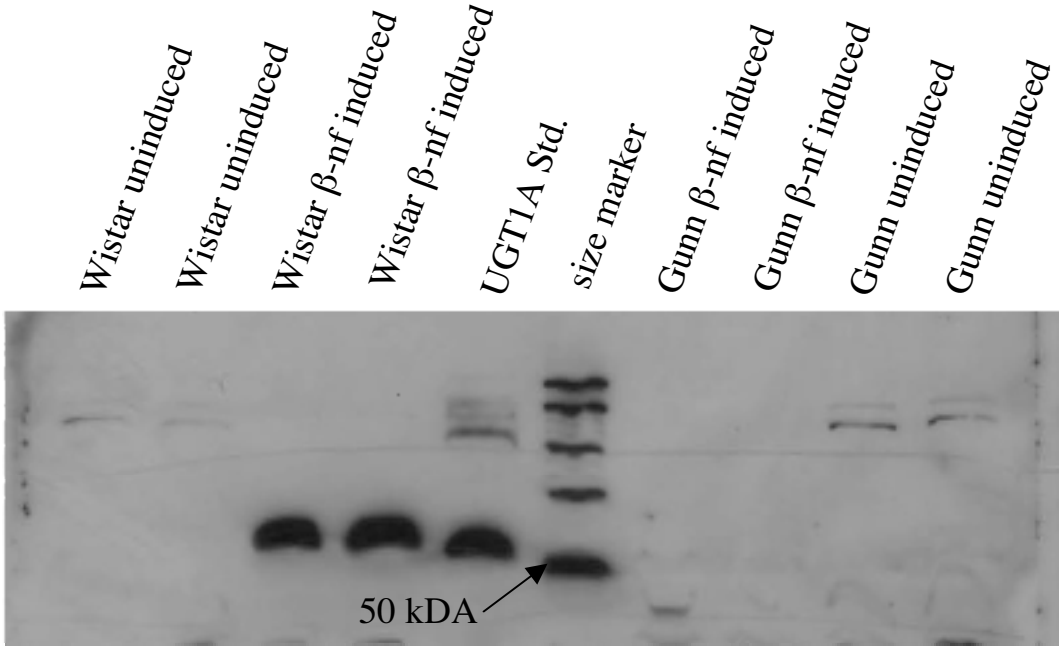
Wistar uninduced
Wistar uninduced
Wistar β-nf induced
Wistar β-nf induced
UGT1A Std.
size marker
Gunn β-nf induced
Gunn β-nf induced
Gunn uninduced
Gunn uninduced
50 kDA

Figure 5

A: Wistar

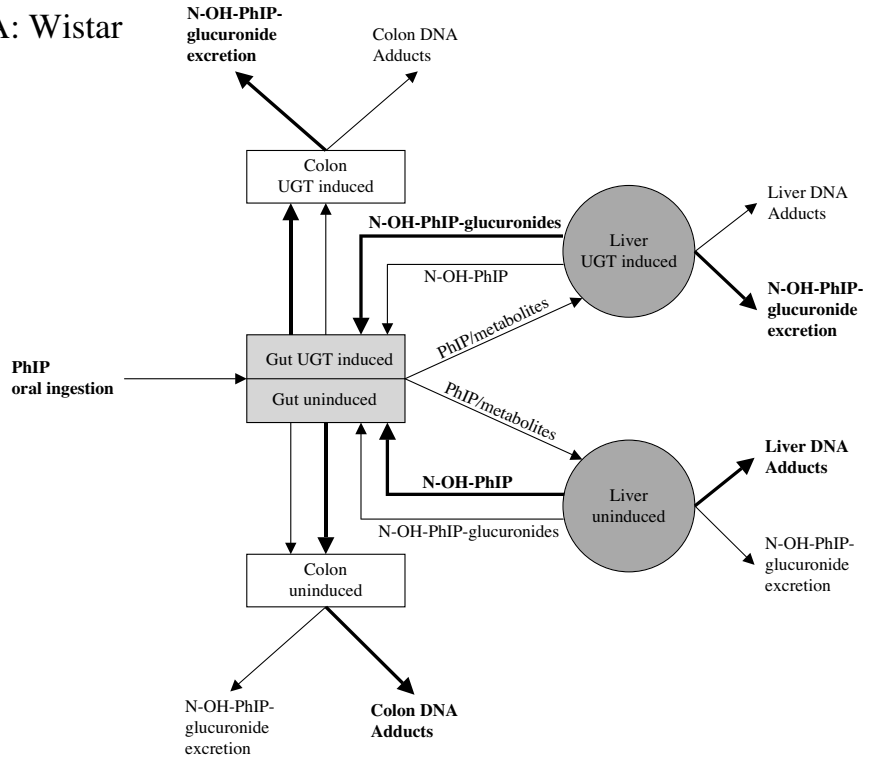

B: Gunn